LASER SURFACE TREATMENT OF A BIODEGRADABLE POLYMER AT VARYING FLUENCES

Anubha Bhatla and Y. Lawrence Yao
Department of Mechanical Engineering
Columbia University
New York, New York

KEYWORDS

Laser, Biodegradable, Polymer, Surface Treatment

ABSTRACT

For biodegradable polymers such as poly (L-lactic acid) (PLLA), material crystallinity has a considerable effect on degradation and physical properties. In this work, the effects of laser fluence of a 355 nm UV Q-switched Nd-YAG laser on the crystallinity and conformation at the surface of PLLA films and the factors affecting the transformation are investigated. Electron microscopy, X-ray diffraction, and infrared spectroscopy are used to study the effects at varying fluences. The melting and crystallization kinetics of PLLA are examined to understand the important parameters that determine the overall crystallinity. Potentially, laser surface treatment at varying fluences can be used to spatially control the generation of a polymer surface with an altered degree of crystallinity. Such a structure may have applications including time-released drug delivery.

INTRODUCTION

Biodegradable polymers, due to their extensive applications and potential have recently generated significant interest. Poly (Ŭ-hydroxy acid) polymers, especially poly (lactic acid) (PLA) and its copolymers are particularly important because they are U.S. FDA approved, have desirable properties, and degrade, primarily hydrolytically, into bioresorbable products. Their applications include drug delivery devices, fixation plates, tissue engineering, packaging, and agriculture.

In biomedical applications, it is important to control polymer surface properties, especially crystallinity. Typical drug delivery devices consist of a drug-infused biodegradable polymer matrix that gradually releases the drug as the matrix degrades hydrolytically, leading to erosion. Drug-release profiles are hence affected by degradation rates, which in turn are a strong function of material crystallinity. Tsuji and Ikada (1998) studied the effect of crystallinity on the PLA degradation and concluded that hydrolysis of PLA chains initiates in the amorphous regions within and between the spherulites. Also, hydrolytic bulk degradation of polyesters shows an initial incubation period, which is disadvantageous in applications

requiring rapid initial drug release. Hence, surface amorphous regions can potentially be used to initiate surface erosion during incubation and hence alter drug-release profiles. Although methods like plasma treatment can affect surface properties, structural modifications have not been attempted, as they are inherently difficult to control spatially. Laser processing of biodegradable polymers has primarily focused on micro and nano scale fabrication, as studied by Kancharla et al. (2001). Laser treatment as a means of surface modification is attractive due to spatial control and the ability to control laser properties to control the affected material depth.

Aguilar et al. (2005) have studied the effects of laser patterning on poly (glycolic acid) (PGA). They observed chemical changes and initial degradation increase without affecting overall degradation time but did not study the reasons for the affected changes. Lazare and Benet (1993) used a single excimer pulse to induce periodic roughness on Mylar (PET) film surface and with ellipsometric measurements showed formation of a surface layer with different optical properties, but the structural changes were not studied. Dunn and Ouderkirk (1990) have also studied excimer laser texturing of crystalline PET and, due to observed increase in refractive index and IR spectroscopy data, suggested that the anisotropy of the surface amorphous layer causes texturing. However, they did not investigate details of the crystal structure changes or factors affecting it.

The focus of this paper is to utilize laser processing to reduce the crystallinity at the surface of PLA films, with the potential to allow for faster surface degradation in the modified regions compared with bulk. Effects of varying fluence on the affected depth are studied. Scanning electron microscopy (SEM), wide angle X-ray diffraction (WAXD), and Fourier transform infrared spectroscopy (FTIR) are used to analyze the morphology and crystallinity changes at the surface. Factors affecting the laser melting and crystallization of PLA are investigated to study the important parameters and reasons for modified crystallinity post-laser irradiation.

MELTING AND CRYSTALLIZATION IN POLY (L-LACTIDE)

To consider the effect of laser processing on PLA, it is important to understand the melting and crystallization characteristics of polymers in general and PLA in particular. High molecular weight PLA is a thermoplastic with a melting temperature of 170–210°C, which makes it suitable for thermal processing. PLA can exist as isomers poly-L-lactide (PLLA) or poly-D-lactide (PDLA), of which PLLA is semicrystalline and can be crystallized by cooling from melt, annealing, and under strain. It is known to crystallize by chain folding, forming lamellae perpendicular to the chain axis. Polymers show a melting transition over a temperature range, with the equilibrium melting temperature (Gibbs-Thompson Equation) varying with the distribution of the lamellar thickness. Nanosecond laser irradiation can cause rapid heating with cooling rates on the order of 10^8 K/s, which are much higher than traditional thermal rates of 10–100 K/s. The total amount of the crystallinity in the material is a function of nucleation and growth, which are a strong function of the cooling rate. In general, in polymers, melting is a fast process completed with low superheating, versus crystallization that is a relatively slower process requiring high supercooling. Crystallization studies of PLLA have shown that the kinetics of melt crystallization of PLLA are relatively slow and hence the possibility of affecting its crystallinity using laser irradiation.

While Wunderlich (1980) has discussed crystallization in detail, nucleation rate is a function of the free energy of nucleation barrier (φG), which is a function of undercooling ($\varphi T = T_m - T_c$; T_m is equilibrium melting temperature and T_c is crystallization temperature) and the free energy of activation (φG_d). Nucleation rate increases rapidly close to glass transition reaching a maximum at $T_c = T_c^*$, which is on the order of 105–110°C in PLLA. During laser processing, large deviations from T_m occur and hence the final development of crystallinity is expected not to be limited by the nucleation barrier, but by growth kinetics. According to the widely accepted Lauritzen-Hoffman Theory (1976), the growth rate, G, of the crystal can be simplified as:

$$G = G_0 \exp\left[-\frac{U^*}{R(T_C - T_\infty)}\right] \exp\left[-\frac{K_g}{T_C \Delta T f}\right] \qquad (1)$$

where K_g is the nucleation constant, $f = 2T/(T_m+T)$ is a factor accounting for heat of fusion change due to deviation from T_m, U^* is the activation energy of segment transport, R is the gas constant, T_∞ is the temperature at which

no motion is seen, and G_0 is the front factor (relatively independent of temperature). In the case of PLLA, primarily regime II growth, i.e., high nucleation rate with low growth velocity is seen during isothermal crystallization.

Laser processing requires a non-isothermal approach to overall crystallization as described by Nakamura, et al. (1972). The heat balance in unit mass can be described by

$$\frac{d\phi(t)}{dt} = \frac{R(T - T_s)}{\Delta H} + \frac{C_p}{\Delta H}\frac{dT}{dt} \qquad (2)$$

where ϕ is the mass fraction of the transformed polymer, ΔH is the heat of crystallization, R is the heat transfer coefficient to surroundings at temperature T_s, and C_p is the mean specific heat of the polymer. The equation can be solved to obtain $T(t)$, the temperature during cooling, and the transformed fraction as a function of time can be simplified to Avrami form as:

$$\phi(t) = 1 - \exp\left\{-\left[\int_0^t K(T(\tau))d\tau\right]^m\right\} \qquad (3)$$

where $K(T) = k(T)^{1/m}$ and $k(T)$ is the isothermal crystallization rate constant and depends on the shape of the growing crystallites and type and number of nuclei formed; and m is the Avrami exponent, which depends on nucleation type and growth geometry.

EXPERIMENTS

Sample Preparation

PLLA pellets with less than 0.01% residual solvent and less than 0.01% residual monomer were obtained from PURAC America. Films of average thickness 15–30 µm were prepared by solvent casting using the method described by El-Amin et al. (2002). Briefly, pellets were dissolved in methylene chloride (0.1 g/3ml, Sigma Aldrich), stirred for three hours, cast in a glass dish, and left to settle for 10 hours at –20°C. The film was cut into 15 mm x 15 mm squares, dried for 24 hours prior to use, and subsequently annealed at 110°C for three hours. Amorphous samples were obtained by melting at 200°C for three minutes and quenching in dry ice.

Experimental Setup and Characterization

The experimental setup (Figure 1) consists of a Q-switched Nd:YAG laser operating at 355 nm in TEM00 mode with pulse duration of 50 ns and a repetition rate of 1 kHz. The laser beam diameter used was 28 µm, scan velocity optimized at 3 mm/s, and the fluence varied from 30-50 J/cm^2. The sample was placed in a holder on synchronized XYZ stages and a 9 mm x 5 mm area laser treated in air. 355 nm wavelength was selected as the photon energy is below the bond breaking energy of C-C and C-H bonds allowing for primarily thermal effects, which are beneficial to induce melting and structural changes as opposed to photochemical bond breakage occurring at shorter wavelengths. Laser parameters were chosen based on the basic finite element (ABAQUS) heat transfer model to identify the melting window below the ablation threshold and experimental optimization. The microstructure of the surface and microtomed sample cross section was observed with the aid of a SEM (JEOL JSM-5600 LV) at voltages of 3–5 kV after gold coating (4–6 min.). For cross-section observation, thicker 300 µm thickness samples were used for ease of microtoming.

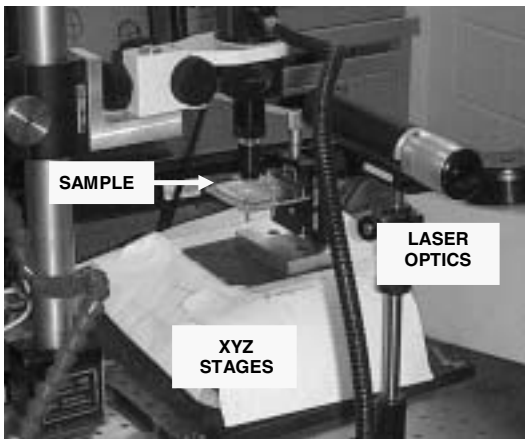

FIGURE 1. EXPERIMENTAL SETUP.

WAXD measurements were carried out using an Inel X-ray diffractometer. Film specimens were exposed to monochromatic Cu KŬ radiation (ə=1.542 Å) at 30 kV and 30 mA. A mass absorption coefficient calculated for PLLA indicates that X-rays penetrate through the bulk of the film.

Thermo-Nicolet FTIR spectrophotometer with ATR (attenuated total reflectance) attachment using a ZnSe crystal (45°) and 4 cm^{-1} resolution was used for measuring the IR spectrum of the samples (averaged over 128 scans) and analyzed by Omnic software. Care was taken to

ensure reproducible pressure between the sample and crystal for a set of experiments, each measurement was repeated at least twice, and ATR correction was applied to normalize the effect of wavelength dependence. The depth of penetration was estimated to be 0.98–2.8 μm in the wave number range from 2000–650 cm^{-1}.

RESULTS AND DISCUSSION

The surface morphology of the solution cast and annealed polylactide films observed under SEM is shown in Figure 2. Spherulitic aggregations that were partly merged were observed and confirmed with the optical microscope.

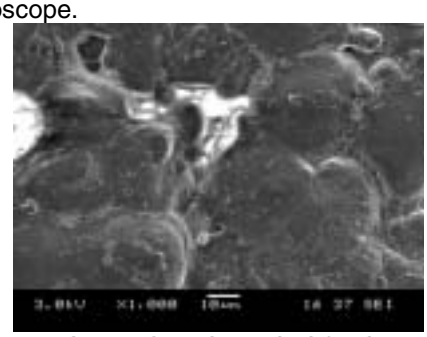

FIGURE 2. SURFACE MORPHOLOGY OF PLLA SAMPLE FILMS AS OBSERVED UNDER SEM.

Crystallinity Modification: WAXD

The crystal structure of PLLA has been well studied and three different crystal modifications are seen; viz the Ŭ, ɓ, and ɔ form, depending on processing conditions. The Ŭ-form is the most commonly observed polymorph with an orthorhombic unit cell with 2 10_3 (3 monomeric units per 10 Å rise) polymeric helices. The unit cell dimensions indicated by Marega et al. (1992) are a = 10.7 Å; b = 6.126 Å, and c = 28.939 Å. The X-ray diffraction profile of untreated, treated (40 J/cm^2), amorphous sample, and background scatter are shown in Figure 3. Crystallinity of the samples was determined based on simplifications of the Ruland Method, as discussed by Alexander (1969). Background scattering was separated and amorphous fraction fit using a Gaussian profile. Mass fraction of the crystalline phase (crystallinity: $\bar{u}_c$) was obtained by dividing the total intensity of the crystalline reflection with the total intensity. Disorder factor due to lattice defects and thermal disorder was not considered. The most prominent peak is seen at 16.7° representing the (110/ 200) reflections and smaller peaks at 14.7° and 19.1° representing the planes with miller indices of (010) and (203), respectively. This agrees with the α-form of PLLA consistent with other observations in literature for solution grown crystals.

Crystallite thickness can be measured using the Scherrer Equation, $t_{hkl} = k\lambda / B_{hkl} \cos\theta$, where t_{hkl} is the crystallite size perpendicular to the plane (*hkl*), *k* is the crystallite shape factor (0.9), λ is the wavelength, B_{hkl} is the width at half-maximum, and θ is the Bragg angle. The crystallite thickness was calculated to be in the range 15–20 nm (110/200 reflection), as seen in Figure 11.

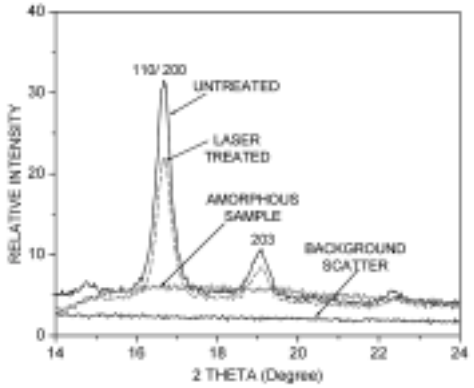

FIGURE 3. WAXD PROFILES OF UNTREATED, LASER TREATED (40 J/CM^2) AND AMORPHOUS SAMPLE AND BACKGROUND SCATTER. NOTE REDUCTION IN 110/200 AND 203 PEAKS.

The WAXD profiles of the crystalline fraction of untreated sample and irradiated at increasing fluences are shown in Figure 4. There is a reduction in the intensity of both (110/200) and (203) peaks which indicates that the laser treatment primarily resulted in reduced order perpendicular to the helical chain direction and hence sample crystallinity.

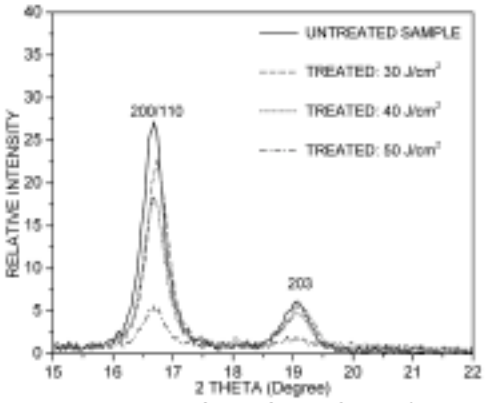

FIGURE 4. WAXD PROFILES INDICATING EFFECTS OF LASER FLUENCE ON THE CRYSTALLINE FRACTION OF PLLA SAMPLE.

Figure 11 indicates the effect of laser fluence on the measured mean crystallinity and crystallite thickness (bars indicate standard errors). The crystallinity of the sample was reduced by 7–8% for lower intensities to almost half at higher fluences. Because WAXD provides integral intensity data from the complete depth of the sample film, this can be attributed both to increased energy input causing melting of crystallites at progressively increasing depths in the sample films and more complete melting at higher temperatures in the surface regions.

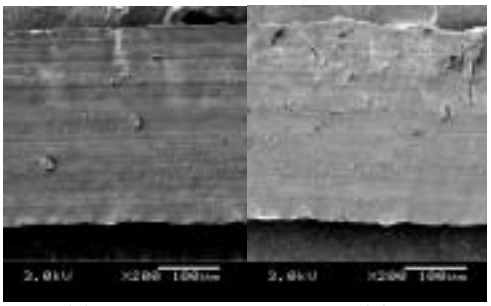

(a) (b)

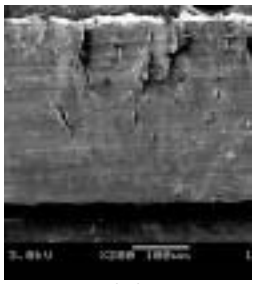

(c)

FIGURE 5. SEM IMAGES OF 300 µm. (a) UNTREATED SAMPLE AND FILMS TREATED AT (b) 30 J/CM^2 AND (c) 50 J/CM^2 INDICATING INCREASED CRAZING WITH FLUENCE.

While the crystallite thickness is not observed to change considerably, mean crystallite thickness reduces at higher fluences which indicates that disruption of structure might stem from partial melting at lower fluence regimes and more complete melting of high melting crystals at higher fluence, causing random displacement. This would explain why no significant broadening occurs in the XRD profiles and the main effect seen on irradiation is a reduction in the measured intensity. Figure 5 shows the SEM images of the untreated 300 µm sample and those treated at 30 and 50 J/cm^2, respectively. While no direct melting regions can be distinguished, it is apparent that there the affected depth increases with increased fluence. Crazing has been widely observed in semi-crystalline polymers and it has been suggested by Friedrich (1983) that crazes are initiated between the amorphous regions zones between the crystal lamella, which is in accordance with our observations.

Conformational Modification: ATR-FTIR

FTIR spectroscopy can provide information regarding chain conformations and crystallinity in semicrystalline polymers. ATR-FTIR spectrum of untreated, laser treated at 30 J/cm^2 and amorphous PLLA film are shown in Figure 6.

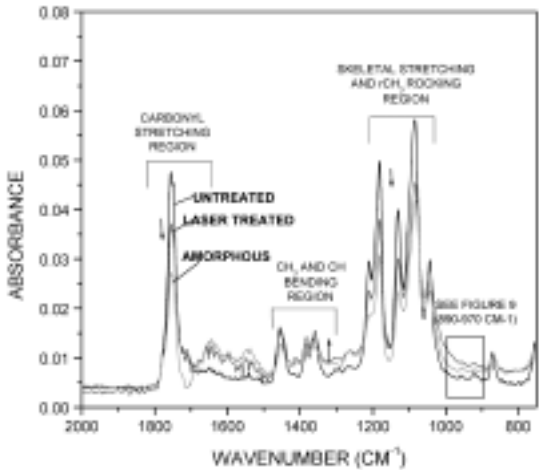

FIGURE 6. FTIR SPECTRA OF UNTREATED, TREATED (30 J/CM^2) AND AMORPHOUS SPECIMENS (2000-700 CM^{-1}) INDICATING IMPORTANT BENDING, STRETCHING AND ROCKING MODES OF PLLA.

It can be seen that the Carbonyl (C=O) stretching region, CH_3 and CH bending region, and skeletal stretching (C-O-C) regions of original crystalline PLLA show sharper peaks with band splitting and a band at 920 cm^{-1} in accordance with observations from Kister et al. (1998). The PLLA monomer, **[-O-CH(-CH$_3$)-C(=O)-]$_n$**, has three skeletal bonds, C-O (ester), O-C$_{\ddot{U}}$, and C$_{\ddot{U}}$-C, with the ester bond assumed to exist always in the *trans* conformation. From minimum energy calculations (Brant et al. 1969), it is seen that four rotational isomeric states are feasible: *tt*, *tg*, *gt*, and *gg* corresponding to *trans* angles of –160° and 160°, and *gauche* angles of –73° and –48°, respectively. The *gt* conformers have the lowest energy and correspond to a 10_3 helix. While the simulated spectrum shows 55% *gt*, 37% *gg* conformers, and 4% each of other bent conformations, experimentally *gg* conformers (a 4_1 helix) are seen to be much lower and more *tt* conformers are seen that give

extended chains but do not challenge the stiffness shown in PLLA chains.

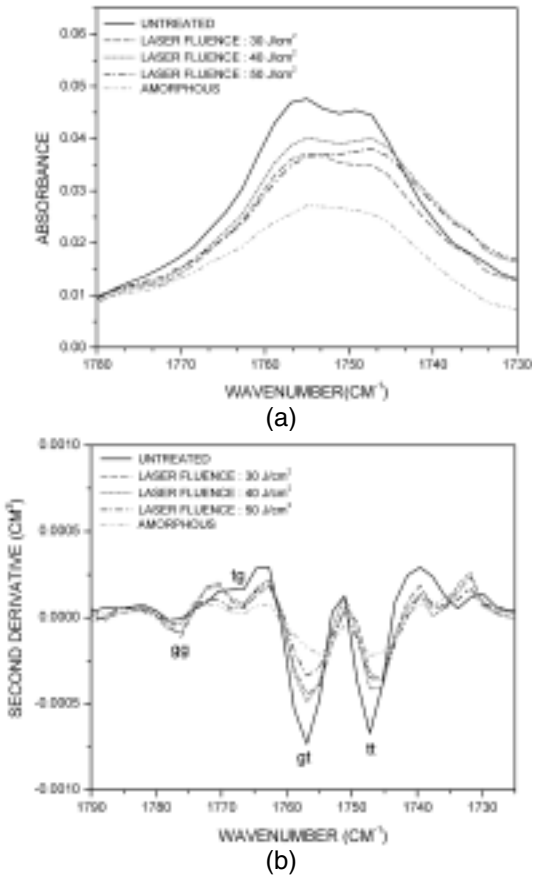

FIGURE 7. (a) C=O STRETCHING AND (b) DERIVATIVE SPECTRUM INDICATING THE PRIMARY CONFORMATIONS AND FACTOR GROUP SPLITTING WITH VARYING FLUENCE.

Following this analysis, Meaurio et al. (2006) have observed that the carbonyl region of PLLA splits into four peaks during crystallization corresponding to different conformations due to intramolecular coupling. The details of the C=O stretching region (1790–1730 cm^{-1}) and the corresponding second derivatives are shown in Figure 7. Pronounced splitting is seen in the original sample with a broad peak in the amorphous sample, and the treated samples show reduced splitting with increasing fluence. Second derivative spectrum indicates peaks at 1776.2, 1766.7, 1757, and 1747 cm^{-1} corresponding to the *gg*, *tg*, *gt*, and *tt* conformers, with the latter two slightly shifted with respect to the transmission spectra peaks observed in literature. Fewer *gg* conformers are observed. The CH_3 and CH bending region in Figure 6 (1250–1400 cm^{-1}) also indicates broadening with irradiation. The skeletal stretching region of PLLA (1050–1260 cm^{-1}) and its derivative spectrum are shown in Figure 8, consisting of asymmetric C-O-C stretching vibrations. These modes split into 1180/1192 and 1210/1222 for the cold crystallized samples, while no/reduced splitting is seen in the laser processed samples, suggesting reduced crystal perfection.

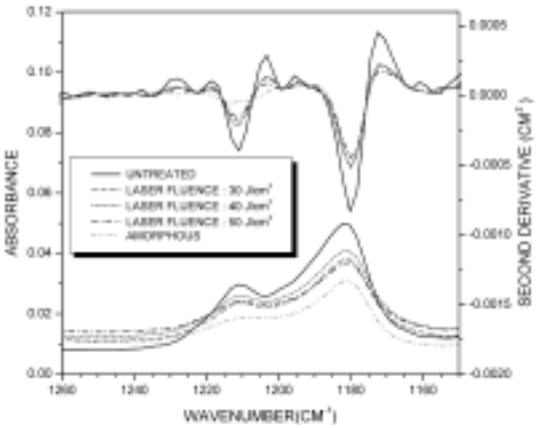

FIGURE 8. FTIR ABSORBANCE AND DERIVATIVE SPECTRUM OF THE SKELETAL STRETCHING REGION OF PLLA.

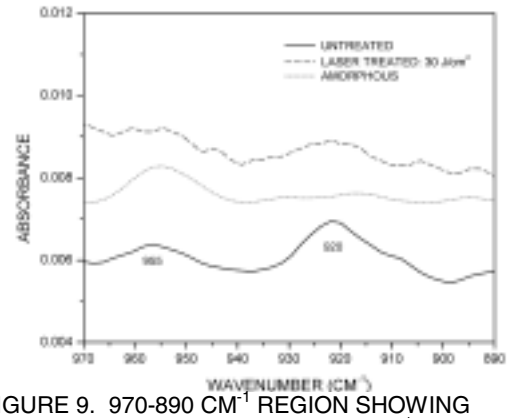

FIGURE 9. 970-890 CM^{-1} REGION SHOWING REDUCTION IN THE BAND AT 920 CM^{-1} AFTER PROCESSING (COUPLING OF THE $_3$C-C STRETCH WITH CH_3 ROCKING MODE).

Figure 9 (970–850 cm^{-1} region) shows that the band at 920 cm^{-1} reduces, while peak at 955 cm^{-1} increases slightly upon laser processing, with significant increase seen at higher fluences. The 920 cm^{-1} band was assigned to coupling of the $_3$C-C backbone stretch with CH_3 rocking mode in 10_3 helical conformation of PLLA in line with Kister et al. (1998).

XRD indicates a 10_3 helical structure (Ŭ-form) of PLLA, and from IR spectra the *gt* conformers

represent the crystalline conformers. Hence, *gt* peaks can be used to understand the effect of laser fluence. Spectral curve fitting was used in Figure 10 for untreated samples to obtain the heights of the peaks at 1757 cm^{-1} (*gt* conformers). Similarly, the effect of fluence is demonstrated by comparing the reduction in peak heights of *gt* conformers (Figure 11), which follows the same trend as WAXD. While this band represents added contributions from the *gt* conformers in the crystal lamellae and the interphase regions, the reduction has to be attributed to conformation changes happening in the crystal domains of the polymer.

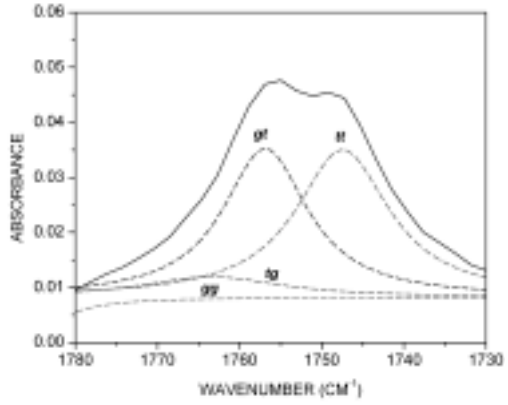

FIGURE 10. CURVE FITTING FOR CONFORMERS IN THE CARBONYL REGION (UNTREATED SAMPLE).

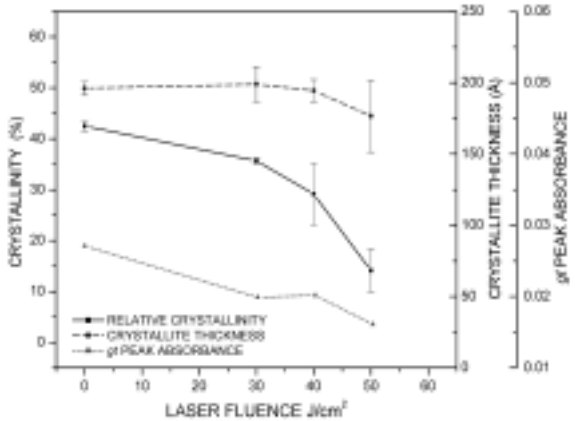

FIGURE 11. EFFECT OF LASER FLUENCE ON CRYSTALLINITY AND CRYSTALLITE THICKNESS OF PLLA (WAXD) AND *gt* PEAK ABSORBANCE FROM CURVE FITTING OF C=O REGION (FTIR SPECTRA).

The reduction is less drastic as compared with the WAXD peaks due to fixed penetration depth of ATR-IR spectrum. However, the reduction in conjunction with reduced lamellar thickness may imply transition from partial to complete melting at higher fluences in the layer at the surface probed by the ATR crystal.

Additional Comments

Due to rapid melting kinetics in polymers with low superheating, the surface of the material would experience melting temperatures and an increase in the affected depths would be expected with increase in fluence due to higher temperatures away from the surface which would explain the variation in crystallinity with fluence seen in WAXD and SEM. In addition, at critical temperatures close to and below the melting point conformational disorder can increase. This along with presence of low melting crystals might contribute to an increase in interlamellar material, leading to partial melting at depths higher than those seen by considering melting temperatures alone. As seen in Figure 11, the reduction in intensity of the *gt* conformer peak is more pronounced at higher fluences and considering that the probed depth is fixed for FTIR (~2 µm) this may indicate that more complete melting is seen at higher fluences in the surface regions. Also, FTIR results do not indicate any new bands suggestive of degradation. At 355 nm, the photon energy, $E = 1245/\lambda = 3.5$ eV, is not enough for direct bond breaking and hence photochemical effects would be expected to be negligible.

The cooling rates during the laser pulse are rapid and, due to considerable rapid undercooling during the pulse duration and considering dependence of nucleation on undercooling $\varphi(\Delta T)$ (section II), nucleation may be considered non-limiting and growth will primarily govern crystallinity evolution. Vasanthkumari and Pennings (1983) have shown that growth in PLLA follows regime II kinetics based on Kg values in Eq. (2). Maximum spherulite growth rates seen are around 130°C (5 µm/min.). In this light, the overall development of crystallinity can be estimated. In the literature, Avrami exponent for PLLA (*m*) is on the order of 3 and *k* values in the range of 5e-8 to 8e-10. From the laser quench rate $T(t)$, the values of $K(T(t))$ in non-isothermal Avrami equation (4) can be obtained. In the future, we expect to obtain actual $T(t)$ values using numerical methods. Considering a single pulse at 1 msec (at 1 kHz), the value of the integral crystallization rate constant in Eq. (3) is expected to be small, contributing to a

small degree of transformation, ū , so that the transformed material would be amorphous.

CONCLUSIONS

It has been shown that nanosecond laser irradiation at 355 nm can be used to reduce the crystallinity of biodegradable polymer L-PLA, and final crystallinity is a function of the fluence. WAXD results show increased reduction in intensities perpendicular to the helical PLLA axis, with reduced overall crystallinity with an increase in fluence. FTIR spectra exhibit broadening, smaller factor group splitting and reduction in *gt* conformers as fluence increases, which also confirms that these conformers primarily crystallize in Ŭ-form. Rapid surface melting, high laser quench rates, and primarily regime II kinetics of PLLA contribute to an overall reduction in crystallinity. Partial melting may be an important contributory factor. Laser surface treatment can potentially allow for an automated process to spatially control the surface morphology and hence degradation associated with different crystallinity at the surface.

ACKNOWLEDGMENTS

Financial support from Columbia University and PURAC America's contribution with PLLA sample material is acknowledged. Prof. J. Koberstein's discussions are sincerely appreciated. Assistance from Prof. Helen Lu's group for sample preparation and Dr. Louis Avila for FTIR equipment are also appreciated. This work used equipment at the Columbia University MRSEC supported by NSF DMR-0213574.

REFERENCES

Aguilar, C.A.; Y. Lu; S. Mao; and S. Chen (2005). "Direct Micro-Patterning of Biodegradable Polymers Using Ultraviolet and Femtosecond Lasers." *Biomaterials* (v26, n36), pp. 7642-7649.

Alexander, L. (1969). *X-Ray Diffraction Methods in Polymer Science*. New York: Wiley-Interscience.

Brant, D.A.; A.E. Tonelli; and P.J. Flory (1969). "The Configurational Statistics of Random Poly(lactic acid) Chains." *Macromolecules* (v2, n3), pp. 228-235.

Dunn, D.S. and A.J. Ouderkirk (1990). "Chemical and Physical Properties of Laser-Modified Polymers." *Macromolecules* (v23, n3), pp. 770-774.

El-Amin S.F. et al. (2002). "Human osteoblast integrin expression on degradable polymeric materials for tissue engineered bone." *Journal of Orthopaedic Research* (v20, n1), pp. 20-28.

Friedrich, K. (1983). "Crazes and Shear Bands in Semi-Crystalline Thermoplastics." *Advances in Polymer Science* 52/53.

Hoffman, J.D.; G.T. Davies; and J.I. Lauritzen (1976). Treatise on Solid-State Chemistry Vol. 3, Chapter 15. New York: Plenum Press.

Kancharla, V. and S.C. Chen (2001). "Laser Micromachining of a Biodegradable Polymer." *Transactions of NAMRI/SME* (Vol. 29), pp. 407-412.

Kister, G.; G. Cassanas; and M. Vert (1998). "Effects of Morphology, Conformation And Configuration on the IR and Raman Spectra of Various Poly(Lactic Acid)s." *Polymer* (v39, n2), pp. 267-273.

Lazare, S. and P. Benet (1993). "Surface Amorphization of Mylar Films with Excimer Laser Radiation Above and Below Ablation Threshold." *Journal of Applied Physics* (v74, n8), pp. 4953-4957.

Marega, C.; A. Marigo; V. Di Noto; and R. Zannetti (1992). "Structure and Crystallization Kinetics of Poly (L-Lactic Acid)." *Makromol. Chem.* (v193, n7), pp. 1599-1606.

Meaurio, E.; N. Lopez-Rodriguez; and J.R. Sarasua (2006). "Infrared Spectrum of Poly(L-lactide): Application to Crystallinity Studies." *Macromolecules* (v39, n26), pp. 9291-9301.

Nakamura, K.; T. Watanabe; K. Katayama; and T. Amano (1972). "Some Aspects of Nonisothermal Crystallization of Polymers. I." *Journal of Applied Polymer Science* (v16, n5), pp. 1077-1091.

Tsuji, H. and Y. Ikada (1998). "Properties and Morphology of Poly (L-Lactide) II." *Journal of Polymer Sci., Part A: Polymer Chem.* (v36, n1), pp. 59-66.

Vasanthakumari, R. and A.J. Pennings (1983). "Crystallization Kinetics of Poly(L-Lactic Acid)." *Polymer* (v24, n2), pp. 175-178.

Wunderlich, B. (1976). *Macromolecular Physics*, Vol. 2, and (1980), Vol. 3. New York: Academic Press.